Babeş-Bolyai University, Cluj-Napoca
Faculty of Physics

BORBÉLY SÁNDOR

PhD thesis Summary

Theoretical study of the interaction between atomic and molecular systems and ultrashort laser pulses

Scientific advisor: prof. dr. LADISLAU NAGY

January 2010

Contents of the Thesis

Keywords

- ultrashort laser pulses

- tunneling / over-the-barrier ionization

- momentum-space strong-field approximation (MSSFA)

- "exact", numerical solution of the TDSE

- hydrogen atom

- positronium

- water

- hydrogen molecule/ molecular ion

- two slit interference

List of publications

- ISI articles

  1. L. Nagy, S. Borbély and K. Póra, *Interference effects in the photoionization of molecular hydrogen*, Phys. Lett. A **327** (2004) 481–489. (impact factor: 1.454)

  2. L. Nagy, S. Borbély and K. Póra, *Interference Effects in the Ionization of Diatomic Molecules*, Braz. J. Phys **36** (2006) 511-514. (impact factor: 0.494)

  3. S. Borbély and L. Nagy, *Study of the interference effects in the ionization of H_2 by the use of two-center wavefunctions*, Rad. Phys. Chem. **76** (2007) 516–520. (impact factor: 0.934)

  4. S. Borbély, L. Nagy, K. Tőkési, *Ionization of the hydrogen atom by intense ultrashort laser pulses*, Phys. Rev. A **77** (2008) 033412. (impact factor: 2.893)

  5. S. Borbély, L. Nagy, K. Tőkési, *Interaction of intense short laser pulses with positronium*, Nucl. Instr. and Meth. B **267** (2009) 386. (impact factor: 0.997)

  6. S. Borbély, G. Zs. Kiss and L. Nagy, *The excitation and ionization of the hydrogen atom in strong laser fields*, Cent. Eur. J. Phys. (in press) doi:10.2478/s11534-009-0150-5. (impact factor: 0.448)

  7. S. Borbély, L. Nagy, K. Tőkési, *Ionization of the water by intense ultrashort half-cycle electric pulses*, Eur. J. Phys. D (submitted in 2009).

- Other articles

  1. S. Borbély and L. Nagy, *Resonance effects in quantum transitions induced by ultrashort laser pulses with high repetition rate*, Studia UBB Physica, **1** (2007) 53-65.

  2. S. Borbély and L. Nagy, *Resonance effects in the photoionization of atoms (molecules)*, MŰSZAKI SZEMLE **41** (2008) 35-39.

  3. S. Borbély, L. Nagy, D. G. Arbó, K Tőkési, *Over-the-barrier ionization of H_2O by intense ultrashort laser pulses*, AIP Conf. Proc. **1080** (2008) 145.

  4. S. Borbély, K. Póra, L. Nagy, *Non-perturbative investigation of the interference effects in the ionization of the H_2 by charge particle impact*, J. Phys. Conf. Ser. **163** (2009) 012067.

Introduction

Nowadays advanced laser facilities can routinely achieve intensities of the order of 10^{15} W/cm^2 and pulse lengths of the order of 10 fs, which corresponds to a few cycles of an electrical field of 800 nm wavelength [1–3]. In the past years research activities have turned to investigations of the interactions between such short and strong pulses with matter. During the interaction of such laser beams and atoms or molecules new and only partially understood processes are taken place. In very a simplified picture, the interaction between atoms and strong, ultrashort laser pulses can be understood using the simple man's three step model [4]. In the first step the atoms are ionized by the external laser field via multiphoton ionization (MPI), tunneling ionization (TI), or over-the-barrier ionization (OBI)(also called direct ionization) depending on the field's parameters. In the second step the free electron wave packet is moving under the influence of the external laser field, while in the third step, depending on the field parameters, the free electron wave packet may return to the vicinity of the parent ion, where it interacts with the ion. In this third step the returning electron wave packet may excite, further ionize the parent ion, or it may be reabsorbed by the parent ion followed by the emission of an energetic photon (high harmonics generation (HHG)).

The subject of the present thesis is the investigation of the direct ionization process, which is the first step of the three step model. The further propagation and the eventual recollision of the free electron wave packet with the parent ion is not the subject of the present work. All the theoretical investigations of the ionization processes are based on the solution of the time dependent Schrödinger equation (TDSE). Since exact analytical solution of the TDSE does not exist even for the simplest system (hydrogen atom in electromagnetic field), there are two possible approaches to solve the TDSE. The first possibility is the direct numerical solution of the TDSE using various techniques. These approaches are "exact" and provide accurate results, but they involve extensive numerical calculations with high computational costs (memory and CPU time). The second possibility is the approximate solution of the TDSE, which has the advantage that involves much less computations, but they provide

less accurate results.

In the first part of the thesis we will present an approximate theoretical approach, which can be considered as viable alternate to Coulomb-Volkov (CV) models. Our theoretical approach is based on the first order iterative solution of the TDSE in momentum space. This approach is closely related to the strong-field approximation (SFA) [5]. The main difference between our method and the SFA is that we perform our calculations in momentum space. Therefore, to distinguish our scheme from the traditional SFA, we call our approach the momentum-space strong-field approximation (MSSFA). The main advantage of this approach stands in its simplicity and in the fact, that the intermediate excited bound states are implicitly included in the ionization dynamics. The main shortcoming of the MSSFA is that it considers the Coulomb interaction between the core and the active electron only as a first order perturbation, which limits the applicability of the model at lower laser field intensities. The theoretical foundations of the MSSFA model are presented in chapter 2, while its viability is tested in chapter 3., where it is applied to describe the ionization of hydrogen type systems by ultrashort laser pulses.

In the second part of the thesis a numerical approach is presented for the solution of the TDSE. In this approach the time dependent wave function of the system is expanded in terms of Volkov wave functions, and for the expansion coefficients an integro-differential equation is established based on the TDSE. The expansion coefficients are discretized on a finite element discrete variable representation (FEDVR) numerical grid and according to the integro-differential equation, they are propagated in time using the Kutta-Merson method. The advantage of the present approach is that the expansion coefficients are coupled only by the Coulomb potential, but this simplification comes with the price that this coupling is not sparse, which significantly complicates the numerical calculations. The main advantage of the approach surface, when it is applied to study the ionization of molecules, where the Coulomb potential is multicentered. These multicentered Coulomb potentials have several singularities (one in each center), and the numerical treatment of these singularities in coordinate space is difficult, because they are not located at the center of the coordinate system. In our numerical approach these Coulomb singularities can be easily eliminated even in the case of the multicenter potentials, where all singularities are reduced to only one.

TDSE in momentum space

In the present chapter the TDSE written in momentum space for atomic systems in external electromagnetic fields is analyzed in detail, and iterative approximate solutions of the TDSE are presented.

General Considerations

The time evolution of atomic systems in the presence of one intense ultrashort laser pulse is investigated. The studied atomic system consist of an active electron moving in an effective Coulomb potential, $V(\vec{r})$, describing the interaction between the active electron and the rest of the atomic system.

In the literature there are two alternate ways [5] to describe theoretically the few-cycle ultrashort laser pulses. The first one specifies the electric field of the pulse, while the second one its vector potential. In the present work we define the linearly polarized laser pulse by its electric component and we use a sine-square envelope function:

$$\vec{E}(t) = \begin{cases} \hat{\varepsilon} E_0 \sin\left[\omega(t - \frac{\tau}{2}) - \frac{\pi}{2}\right] \sin^2\left(\frac{\pi t}{\tau}\right) & \text{if } t \in [0, \tau] \\ 0 & \text{elsewhere} \end{cases}, \tag{1}$$

where $\hat{\varepsilon}$ is the polarization vector, ω is the frequency of the carrier wave, τ is the pulse duration, and E_0 is the strength of the laser field. The shape of a typical pulse used in the present calculations is presented on Fig. 1.

The Hamiltonian of the studied atomic system is expressed as

$$\hat{H} = \frac{\hat{p}^2}{2} + \vec{r} \cdot \vec{E}(t) + V(\vec{r}), \tag{2}$$

where $\vec{r} \cdot \vec{E}(t)$ is the interaction potential between the active electron and the laser pulse in length gauge.

Using expression (2) for the Hamiltonian, the TDSE describing the time evolution of the active electron is written as

$$i\frac{\partial}{\partial t}\Psi(\vec{r}, t) = \left[\frac{\hat{p}^2}{2} + \vec{r} \cdot \vec{E}(t) + V(\vec{r})\right]\Psi(\vec{r}, t), \tag{3}$$
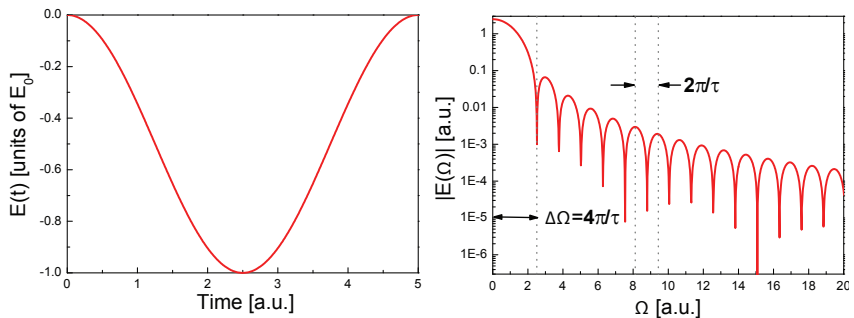
Figure 1: The shape of the pulses in time (a) and in frequency domain. The parameters of the pulse are: $\omega = 0.05$ a.u., $E_0 = 1$ a.u. and $\tau = 5$ a.u.

where $\Psi(\vec{r}, t)$ is the time-dependent wave function. In the present approach the wave function is searched in the following form

$$\Psi(\vec{r}, t) = \int d\vec{k}\, c(\vec{k}, t) \Psi_V(\vec{k}, \vec{r}, t), \tag{4}$$

with $\Psi_V(\vec{k}, \vec{r}, t)$ being the Volkov wave functions. By substituting the time-dependent wave function of Eq. (4) into the TDSE given by Eq. (3) the following integro-differential equation for the $c(\vec{k}, t)$ expansion coefficients can be obtained

$$\frac{\partial}{\partial t} c(\vec{k}, t) = -\frac{i}{(2\pi)^3} e^{\frac{i}{2}\left[k^2 t + 2\vec{k}\cdot\vec{F}(t)\right]} \int d\vec{p}\, c(\vec{p}, t) e^{-\frac{i}{2}\left[p^2 t + 2\vec{p}\cdot\vec{F}(t)\right]} I(\vec{p} - \vec{k}), \tag{5}$$

where

$$I(\vec{s}) = \int d\vec{r}\, V(\vec{r}) e^{i\vec{s}\cdot\vec{r}} \tag{6}$$

is the Fourier transform of the Coulomb potential.

Regardless of the method used to solve Eq. (5), an initial condition is needed:

$$c(\vec{k}, t = 0) \equiv c^{(0)}(\vec{k}) = \frac{1}{(2\pi)^3} \left\langle e^{i\vec{k}\cdot\vec{r}} \mid \psi_i(\vec{r}) \right\rangle, \tag{7}$$

where $\psi_i(\vec{r})$ is the initial state wave function.

Volkov solution

The simplest possible way of solving Eq. (5) is by neglecting completely the Coulomb potential ($V(\vec{r}) = 0$), which can be considered as a zeroth order iterative solution of Eq. (5):

$$c(\vec{k}, t) = c(\vec{k}, t = t) \equiv c^{(0)}(\vec{k}). \tag{8}$$

This approximate solution in the literature is known as the Volkov or sudden SFA model [6].

MSSFA solution

In most cases, the Volkov model (see Eq. (8)) does not provide accurate results, and higher order approximations are needed. In the first order iterative approximation, Eq. (5) can be given as follows:

$$\frac{\partial}{\partial t} c^{(1)}(\vec{k}, t) = -\frac{i}{(2\pi)^3} e^{\frac{i}{2}\left[k^2 t + 2\vec{k}\cdot\vec{F}(t)\right]} \int d\vec{p}\, c^{(0)}(\vec{p}) e^{-\frac{i}{2}\left[p^2 t + 2\vec{p}\cdot\vec{F}(t)\right]} I(\vec{p} - \vec{k}). \tag{9}$$

The advantage of this approach is that it eliminates the direct coupling between the expansion coefficients $c(\vec{k}, t)$, making easier and faster the solution of Eq. (5). Our present approach is similar to the SFA employed by Milošević *et al* [5]. Therefore, to distinguish our scheme from the traditional SFA, we call our model the momentum-space strong-field approximation (MSSFA).

Ionization probability densities

Using plane waves to describe the free electronic states with momentum $\vec{k}$, the ionization probability density can be calculated as follows:

$$\frac{dP}{d\vec{k}} = (2\pi)^3 \left| c\left(\vec{k} - \vec{A}(\tau), \tau\right) \right|^2. \tag{10}$$

The plane wave functions are not orthogonal to the bound wave functions, thus the ionization probability densities calculated based on Eq. (10) contain the contribution of the bound states. The results may be improved by removing these bound states from the time-dependent wave function using the the Gram-Schmidt algorithm.

Application of the MSSFA model

In the first part of this chapter the accuracy of the MSSFA is verified by applying it to study the ionization of the hydrogen atom by ultrashort laser pulses. In the second part of the chapter the MSSFA and VOLKOV models are extended in order to describe the ionization of the hydrogen type systems. A general scaling law valid for the ionization probability densities is also derived.

Ionization of the hydrogen atom

Our theoretical approaches, MSSFA and VOLKOV models, were applied to study the ionization of the hydrogen atom in the over-the-barrier regime [7]. The ionization process in this regime is considered to be a classical one, and it is believed that it can be described well by classical models like the classical trajectory Monte Carlo method (CTMC). Where "exact" published data [8] are not available, CTMC results will be used as reference. Beside testing the validity of our MSSFA approach we also studied the effect of the Coulomb potential during, and after the laser pulse by analyzing the angular distribution of the free electrons at given energies and the ionization probability densities.

Results and Discussions

Calculations were performed using laser pulses with duration τ of 3 a.u., 5 a.u. and 10 a.u. at two different field intensities ($E_0 = 1$ a.u. and $E_0 = 10$ a.u.). The frequency of the carrier wave is fixed at $\omega = 0.05$ a.u. These pulse parameters limits the value of the Keldysh parameter below 0.05, which are characteristic values for the over-the-barrier ionization.

The double-differential ionization probability densities calculated using the Volkov model (VOLKOV), MSSFA, and CTMC [7] models are presented in Fig. 2, where they are plotted as a function of the electron energy and ejection angle. At first sight one may observe that at
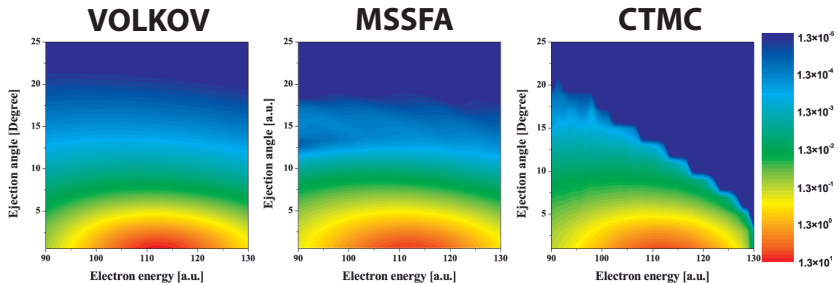
Figure 2: Two-dimensional ionization probability density in the yOz positive semi-plane as a function of the electron energy and ejection angle at fixed laser pulse parameters: $\omega = 0.05$ a.u., $\tau = 5$ a.u. and $E_0 = 1$ a.u.

a large scale all three models predict the same probability densities. In each approach the electrons are ejected with maximum probability along the polarization vector $\hat{\varepsilon}$ with energy around the value $\vec{A}(\tau)^2/2$, which is gained by the momentum transfer $\vec{A}(\tau)$ from the external laser field.

After a detailed analysis, however, important differences can be observed. In the case of the MSSFA and CTMC models the maxima of the predicted probability densities are shifted toward smaller energies. This shift is caused by the Coulomb attraction during the ionization between the active electron and the rest of the system.

The ionization spectra are calculated from the double differential ionization probability densities by integrating over the ejection angle. Figure 3 shows the dP/dE probability densities calculated using the MSSFA, VOLKOV, and CTMC models along with the results of TDSE and CV calculations obtained by Duchateau et al. [6]. The accuracy of the MSSFA and CV results is measured by the agreement with the TDSE results considered to be the best.

A good agreement between MSSFA and TDSE results was found at high laser field intensities (see figure 3 (a)), where the momentum transfer was high, while at lower intensities with low momentum transfer the agreement was acceptable (see figure 3 (b)), comparable with the agreement between the CV and TDSE results. It was shown that except for the case of low momentum transfer, the MSSFA model provides better results than the CV model. The main deficiency of the MSSFA model is that in the case of low momentum transfer the plane waves used for the final state are inaccurate.
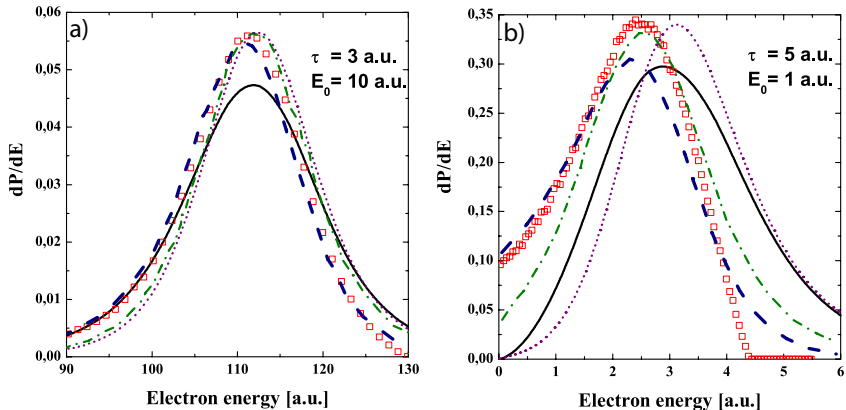
Figure 3: Ionization probability density as function of the electron energy. Solid line: MSSFA. Dotted line: VOLKOV. Squares: CTMC. Dashed line: TDSE [6]. Dash-dotted line: CV [6].

Dissociation of the positronium

The recent development of the positron physics [9,10] made available the experimental investigation of the interaction between the positronium and short laser pulses [9]. The ionization of positronium in intense laser fields was studied by several groups [11,12]. These studies are mainly focusing on the multiphoton and above-threshold ionization (ATI) [12]. The investigation of the ionization spectra in the collisional regime is a subject of interest, due to the fact that the underlying ionization mechanism is completely different from the multiphoton and ATI ionization mechanisms. We have studied theoretically the dissociation of the positronium using the VOLKOV, MSSFA and CTMC models [13]. In the framework of the VOLKOV model we have derived the following analytical formula for the ionization probability density:

$$\frac{dP}{d\vec{k}} = (2\pi)^3 \left(\frac{q}{\pi}\right)^5 \frac{1}{\left[q^2 + \left(\vec{k} + \vec{A}(\tau)\right)^2\right]^4}, \tag{11}$$

where $q = \mu Z_{eff}$ with μ being the reduced mass of the positronium and Z_{eff} the effective charge of the core. From Eq. (11) two scaling relations of the ionization probability density can be extracted:

15
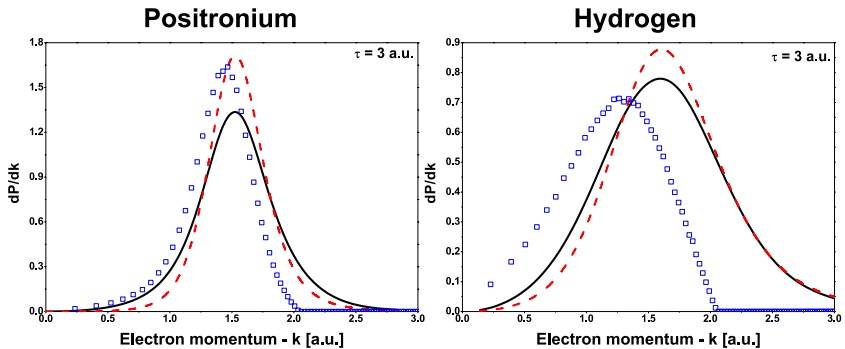
Figure 4: Ionization probability densities as a function of electron momentum. Solid line: MSSFA. Dashed line: VOLKOV. Squares: CTMC

- The photoelectrons are ejected with maximum probability with momentum $\vec{k} = \vec{A}(\tau)$.

- The width of the photoelectron's distribution is directly proportional with μ and Z_{eff}

The validity of these scaling law was tested by calculating the ionization probabilities in the framework of the MSSFA and CTMC models. On figure 4 can be observed that the first scaling law is no longer valid in the case of the MSSFA and CTMC models, because the position of the ionization probability's maximum is also influenced by the Coulomb potential which was neglected in the VOLKOV model. As shown in table 3.1, the validity of the second scaling law is also confirmed by the MSSFA and CTMC calculations.

Table 3.1: The FWHM values of the ionization probability curves presented on Fig. 4.

	MSSFA			Volkov			CTMC		
	H	H/2	Ps	H	H/2	Ps	H	H/2	Ps
$\tau = 3$	1.164	0.582	0.632	0.998	0.449	0.507	1.039	0.519	0.515
$\tau = 5$	1.230	0.615	0.668	1.011	0.505	0.508	1.038	0.519	0.506
$\tau = 10$	1.229	0.614	0.692	1.017	0.508	0.509	1.090	0.545	0.512

Numerical solution of the TDSE

In the first part of this chapter we have presented the numerical methods, which we used during the numerical solution of the TDSE. We have focused on the concept of the FEDVR grid on which the $c(\vec{k}, t)$ expansion coefficients are discretized. Along with the numerical grid, we also discussed the properties of the explicit time propagation methods, which we used during the propagation of the expansion coefficients. In the last part of the section the efficiency of the MPI parallelization is presented along with the performed convergence tests.

The numerical grid

One of the most important part of an "exact" numerical approach is the underlying numerical grid on which the TDSE is discretized. In the present approach a finite element discrete variable representation (FEDVR) grid is used. The FEDVR approach is based on the finite element (FE) method, which implies the division of the configuration space into finite elements. In each finite element the wave function is expressed using a local discrete variable representation (DVR) basis (see figure 5). This way the flexibility of the FE representation is combined with the advantages of the DVR. To ensure the continuity of the wave function the starting and ending points of the neighboring local subgrids must overlap.

The time propagation

The other important element of the "exact" numerical solution is the time propagation of the wave function on the chosen numerical grid. In the present approach the expansion coefficients are propagated in time using the Kutta-Merson method. The estimated relative error after each time step in each gridpoint was calculated, and the maximum of these
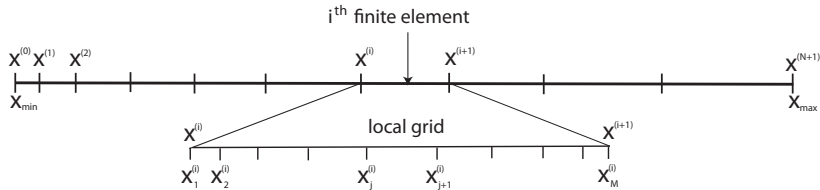
Figure 5: One dimensional FEDVR grid
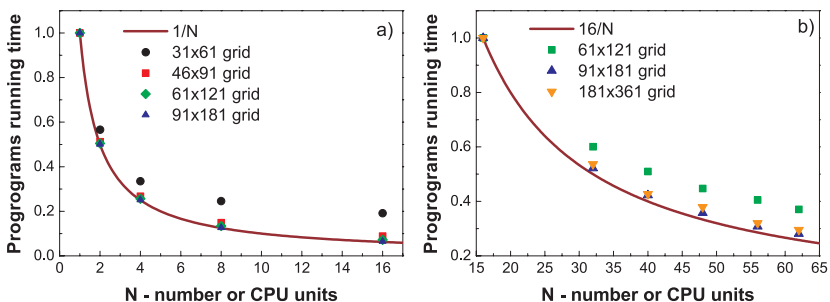
Figure 6: The program's running time as a function of the number of CPU cores used for different radial grids. The measurements were performed (a) on a 16 CPU core machine with shared memory, and (b) on a cluster containing 88 CPU cores where the individual machines are connected via Myrinet network cards.

values (ϵ_m) was considered as the error estimate of the time step. The length of each time step was chosen in such a way, that the relative error estimate (ϵ_m) was smaller than the fixed error tolerance (ϵ_{tol}).

The parallelization of the numerical code

During the numerical solution of Eq. (5) in each time step the most CPU time is needed for the calculation of the integral, which couples the expansion coefficients. For each gridpoint one coupling integral needs to be calculated. These integrals can be calculated independently of each other, giving us the possibility of parallelization. In practice these integrals are calculated parallel on different CPU cores, and after that the obtained values are shared between the cores. The communication between

the cores is realized using the OpenMPI library, which is an open-source implementation of the MPI-2 standard. The efficiency of the parallelization was tested using up to 62 processors (see figure 6).

The convergence of the TDSE results

The reliability of a numerical method is ensured if the produced results are convergence, i.e. they are not changing by the modification of the numerical parameters. The most important outcome of a numerical solution of the TDSE is the time-dependent wave function, which later is used to calculate physical observables. If the convergence of the time-dependent wave function is ensured, in our case of the $c(\vec{k}, t)$ expansion coefficients, then the convergence of the calculated physical quantities is automatically ensured. The precision and the convergence of the expansion coefficients at the end of the simulation, beside the chosen numerical grid and time propagation method, is mainly influenced by the following three parameters:

i) ϵ_{tol} - the value of the time propagation error tolerance

ii) k_{max} - the size of the simulation box

iii) N_{fun}/dk - the density of the numerical grid with N_{fun} being the number of DVR basis functions and dk being the size of the finite elements.

The convergence of the numerical results is also influenced by the laser pulse parameters. Longer laser pulse needs more numerical propagation time steps and it can accumulate more numerical errors. Higher laser pulse intensity implies higher momentum transfer by the laser field to the electron, indicating larger simulation box in a numerical treatment. So, if the convergence of the results is verified for the longest and most intense laser pulse used in the present calculations, then the convergence for shorter and/or less intense pulses is automatically ensured.

TDSE applied to hydrogenic type systems

In the first part of the chapter our TDSE approach is tested by applying it to study the excitation and ionization of the hydrogen atom, while in the second part of the chapter the ionization of the water molecule is investigated within the framework of the hydrogenic approximation.

The ionization and excitation of the hydrogen atom

In order to test our numerical approach, we have investigated the behavior of the hydrogen atom during its interaction with short laser pulses [14]. In the present TDSE approach the time-dependent wave function is discretized on a FEDVR numerical grid, while it is propagated in time using the Kutta–Merson method.

Studying the occupation probabilities of the $2s$ and $2p$ orbitals, we have observed that the $1s \rightarrow 2p$ transition occurs much earlier than the $1s \rightarrow 2s$ one. This can be explained by the fact, that the $1s \rightarrow 2s$ transition needs minimum two photons, while the $1s \rightarrow 2p$ can be produced by one. Analyzing the occupation probability of the excited bound electronic states their importance in the ionization process was identified in accordance with [15].

The ionization probability densities were also calculated and the important ionization mechanisms were identified. In the case of high intensities, the electrons were mostly ionized by the tunneling and the over-the-barrier mechanisms. However, single photon ionization was also observed.

We have compared our calculated ionization probability densities with other "exact" theoretical calculations, and a good agreement was found. Some discrepancies occur for electron ejected with low energies, but these can be corrected by using the exact Coulomb wave functions for the description of the final state.

Ionization of the water

Due to the recent development of laser technology ultrashort laser pulses are widely used in medical research [16] and applications [17]. In most of these applications the external laser pulse interacts with biological tissue containing mainly water. Therefore, most of the processes induced by the ultrashort laser pulses in biological tissues can be explained based on the investigation of the interaction between the H_2O molecule and the external laser field. It was recently shown experimentally that in the ultrashort regime (< 10 fs) the molecular dissociation is negligible [18], and the dominant process is ionization with recollision. Furthermore, it was verified [18], that in the ultrashort regime the main ionization process is the single ionization. The lack of the experimental and theoretical investigations of the ionization of the water in the ultrashort regime calls for further studies. In the present work calculations for the ionization of the water molecule by intense half-cycle electric pulses were presented [19]. Single active electron classical and quantum-mechanical models were employed in the framework of the hydrogenic approximation. In the hydrogenic approximation the $1b_1$ electrons are initialized on a $2p_z$ hydrogenic orbital. The effective charge of the core (Z_{eff}) is calculated using the experimental value of the ionization energy $E_i = 0.463$ a.u. Calculations were performed using electric pulses with duration τ of 1 a.u., 3 a.u., and 5 a.u. at two different field intensities ($E_0 = 0.44$ a.u. and $E_0 = 1$ a.u.). Ionization probability densities are calculated based on Eq. (10) using the TDSE and VOLKOV $c(\vec{k}, t)$ expansion coefficients along with the orthogonalized TDSE (TDSE-O model) and Volkov (VOLKOV-O model) $c_\perp(\vec{k}, t)$ expansion coefficients. The CTMC ionization probability densities are calculated from the simulated classical trajectories. The probability densities predicted by quantum mechanical and classical models are qualitatively the same (see figure 7). In each approach the electrons are ejected with maximum probability along the polarization vector with momentum value around $\vec{A}(\tau)$, which is the momentum gained by the electrons from the external electric field. A double-peak structure in the ionization probability densities can be observed applying both the Volkov and TDSE models. This is the imprint of the double lobe structure of the initial state wave function. In the TDSE-O and VOLKOV-O probability densities a parallel "ridge" structure was observed, which were identified as single-photon ionization peaks attributed to the shape of the half-cycle pulse. The ionization spectra can be calculated from the ioniza-
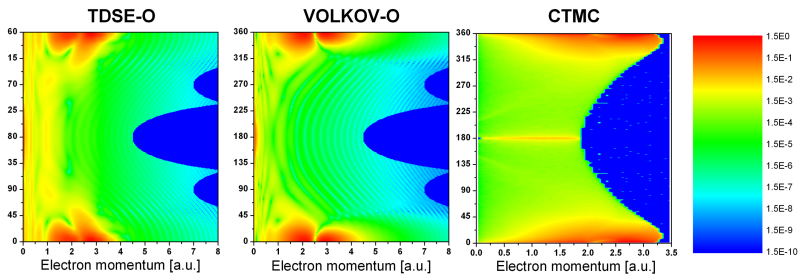
Figure 7: Ionization probability densities in the yOz plane as a function of the electron momentum and ejection angle (measured from the polarization vector $\hat{\varepsilon}$, which coincides with the Oz axis) for pulse parameters $E_0 = 1$ a.u. and $\tau = 5$ a.u.

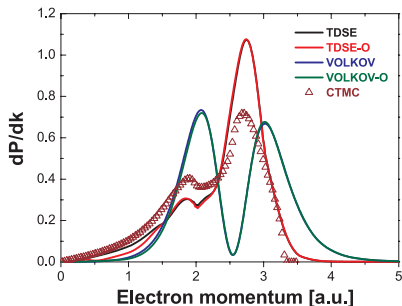tion probability density by integrating over the electron ejection angles. Both the TDSE and VOLKOV models provide qualitatively the same results. In both cases, the dP/dk curve has two maxima around the same electron momenta. Beside these similarities, significant discrepancies exist. In the case of the Volkov model both maxima have the same hight, while in the case of TDSE model the first maximum is considerably smaller than the second one. This difference in the hight of the maxima can be also observed for the CTMC model and can be explained as a result of the

Figure 8: Ionization probability densities as a function of electron momentum at laser pulse parameter $E_0 = 1$ a.u., $\tau = 5$ a.u.

Coulomb interaction between the core and the electron, which is absent for the Volkov model. We found agreement between the CTMC and TDSE-O results (see figure 8) only for pulses with high net momentum transfer toward the active electron.

Ionization of molecules

In this chapter the ionization of the hydrogen molecule and of the hydrogen molecular ion are studied in the framework of the single active electron approximation (SAE) approximation using the VOLKOV and TDSE models. Due to the two center character of the molecules interference effects in the ejected electrons spectra appear. In a simplified picture the nuclei of the molecule can be considered as electron sources and electrons from these two sources may interfere in the continuum leading to oscillations in the ionization probability density. These interference effects for photoionization were first predicted by Cohen and Fano [20] in 1966. Much later, these were experimentally evidenced by Stolterfoht
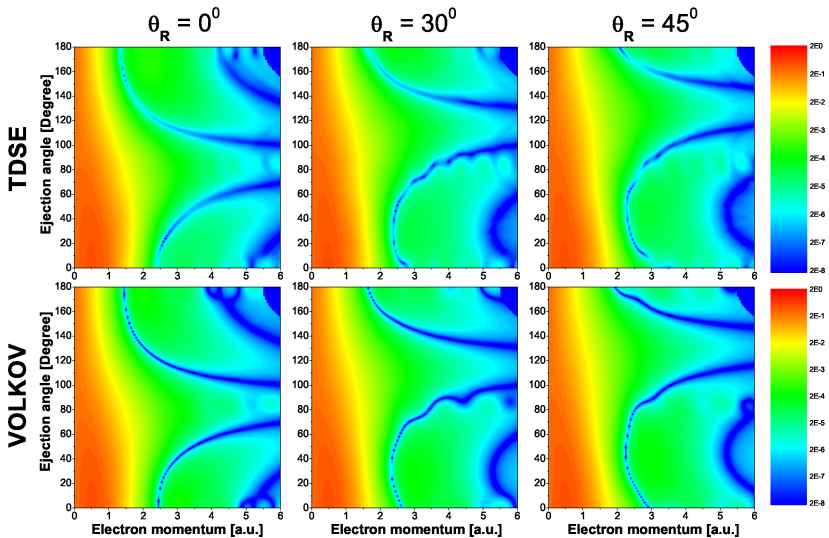

Figure 9: Ionization probability densities as a function of electron momentum calculated for the ionization of the H_2^+ by ultrashort laser pulses. The electron ejection angle and the molecular axis orientation (Θ_R) is measured from the laser field polarization vector.
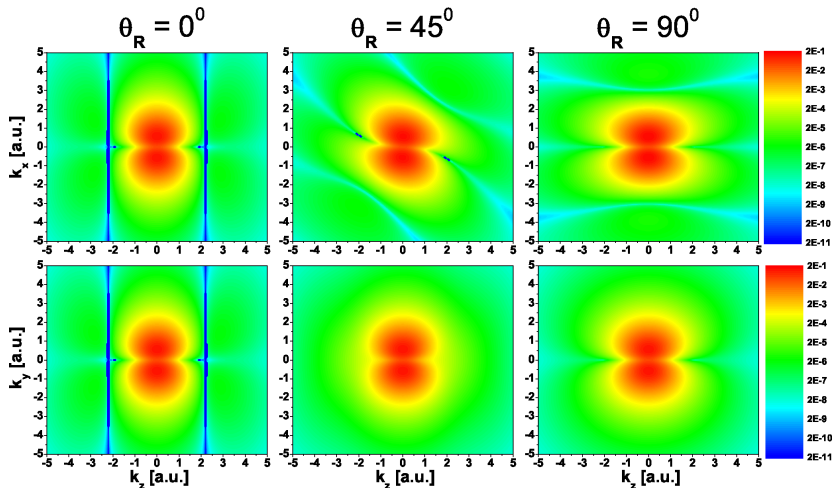
Figure 10: Ionization cross sections in the xOz and yOz planes as a function of the momentum components of the ejected electrons at different molecular axis orientations θ_R

et. al. [21] during the ionization of the H_2 molecule by charged particle impact, which triggered the extensive experimental and theoretical investigation of these interference effects for both photon [22, 23] and charged particle impact [21, 24, 25] ionization. In our previous works [24, 26, 27] we have studied these interference effects in the perturbative regime using different radiation gauges and including partial wave analysis. In this work we have studied these interference effects in the non-perturbative regime using the TDSE and VOLKOV models, which were applied to describe the ionization by both photon and charged particle impact. In the ionization probability densities calculated using the TDSE and VOLKOV models deep minima can be observed (see figure 9), which is the direct evidence of the destructive interference. Here a good agreement between the TDSE and VOLKOV models was observed in the prediction of the interference minima. These minima are defined by the zero values of expression $\cos\left[\vec{R}_0 \cdot \left(\vec{k} - \Delta\vec{p}\right)\right]$, which is in agreement with the empirical formula derived by Stolterfoht et. al. [21]. In the case of charge particle impact ionization for each impact parameter one electric pulse can be as-

sociated [28, 29]. By using these electric pulses the ionization probability densities can be calculated in the framework of the VOLKOV and TDSE models. In order to be able to compare our results with experimental data we need to calculate the ionization cross sections, which is obtained from the ionization probability densities by integrating over all possible impact parameters. As we have shown in figure 10 that this impact parameter integration "destroys" the deep interference minima, with the exception of the xOz plane defined by the molecular axis and the charged particle's impact direction. This result may be usefull in designing new experiments to investigate the ionization of the H_2 molecule with fixed molecular axis orientation, because it exactly tells where one needs to search for the direct evidence of the interference effects. All the experiments on the ionization of the H_2 molecule by fast charged particle impact were performed using randomly oriented molecules, which average out the deep interference minima in the cross sections observable on figure 10. After this averaging the interference effects can not be observed directly in ionization probability density, but its imprint still exists and indirectly it can be emphasized by dividing the half of the molecular ionization cross section with the atomic cross section. The atomic cross section is calculated for a model hydrogen atom with effective charge equal with the effective charge of the nuclei of the molecule.

Conclusions

In the present thesis we have studied theoretically the direct ionization of atoms and molecules by intense ultrashort laser pulses. The main properties of the ionization process, and the theoretical models, which are commonly used to study this process, are presented in chapter 1. In our investigations we have used two different theoretical models, which are based on the solution of the time dependent Schrödinger equation.

The first theoretical model, the MSSFA model, is based on the approximate (first order iterative) solution of the TDSE. The MSSFA model is presented in chapter 2, while in chapter 3 it is applied to study the ionization of the hydrogen type atomic systems. In the literature the CV models are considered to be most efficient ones used to describe the direct ionization in intense laser fields. We found out that our MSSFA approach provides more accurate results with considerable less computations than the CV model if the laser pulse is strong and the momentum of the ejected electrons is high. We also found, that the width of the ionization probability density is directly proportional with the effective charge of the core and with the reduced mass of the hydrogen type system.

The second theoretical model, the TDSE model, is based on the "exact" numerical solution of the TDSE in momentum space. The details of our numerical approach are presented in chapter 4, while its precision is tested in chapter 5, where it is applied to study the ionization of the hydrogen type systems, and an excellent agreement was found with other "exact" calculations [6]. In chapter 7 the TDSE model was applied to study the ionization of homonuclear diatomic molecules by photon and charged particle impact. In both cases we have observed deep minima in the ionization probability densities, which is the clear evidence of the destructive interference. In the case of the charged particle impact ionization we have also shown that in the experimentally measurable ionization cross section these deep interference minima are averaged out by the impact parameter integration with the exception of the xOz plane defined by the molecular axis and by the direction of the projectile.

Bibliography

[1] T. Brabec and F. Krausz. *Rev. Mod. Phys.* (2000) **72** 545–591.

[2] B. Schenkel, J. Biegert, U. Keller, C. Vozzi, *et al. Opt. Lett.* (2003) **28** 1987–1989.

[3] M. Y. Shverdin, D. R. Walker, D. D. Yavuz, G. Y. Yin, *et al. Phys. Rev. Lett.* (2005) **94** 033904.

[4] P. B. Corkum. *Phys. Rev. Lett.* (1993) **71** 1994–1997.

[5] D. B. Milošević, G. Paulus, D. Bauer, and W. Becker. *J. Phys. B-At. Mol. Opt.* (2006) **39** R203–R262.

[6] G. Duchateau, C. Illescas, B. Pons, E. Cormier, *et al. J. Phys. B-At. Mol. Opt.* (2000) **33** L571–L576.

[7] S. Borbély, K. Tőkési, and L. Nagy. *Phys. Rev. A* (2008) **77** 033412.

[8] G. Duchateau, E. Cormier, and R. Gayet. *Eur. Phys. J. D* (2000) **11** 191.

[9] P. Baling, D. Fregenal, T. Ichioka, H. Knudsen, *et al. Nucl. Instr. and Meth. B* (2004) **221** 200.

[10] S. Brawley, J. Beale, S. Armitage, D. Leslie, *et al. Nucl. Instr. and Meth. B* (2008) **266** 497.

[11] L. B. Madsen and P. Lambropoulos. *Phys. Rev. A* (1999) **59** 4574–4579.

[12] V. Rodríguez. *Nucl. Instr. and Meth. B* (2006) **247** 105.

[13] S. Borbély, K. Tőkési, and L. Nagy. *Nucl. Instr. Meth. B* (2009) **267** 386–389.

[14] S. Borbély, G. Z. Kiss, and L. Nagy. *Cent. Eur. J. Phys.* (2010) **in press**.

[15] V. D. Rodríguez, E. Cormier, and R. Gayet. *Phys. Rev. A* (2004) **69** 053402.

[16] H. Hirase, V. Nikolenko, J. H. Goldberg, and R. Yuste. *J. Neurobiol.* (2002) **51** 237–247.

[17] I. Ratkay-Traub, T. Juhasz, C. Horvath, C. Suarez, *et al. Opthalmology Clinics of North America* (2001) **14** 347–355.

[18] D. Mathur, F. A. Rajgara, A. K. Dharmadhikari, and J. A. Dharmadhikari. *Phys. Rev. A* (2008) **78** 023414.

[19] S. Borbély, K. Tőkési, and L. Nagy. *Eur. J. Phys. D* (2010) **submitted**.

[20] H. D. Cohen and U. Fano. *Phys. Rev.* (1966) **150** 30–33.

[21] N. Stolterfoht, B. Sulik, V. Hoffmann, B. Skogvall, *et al. Phys. Rev. Lett.* (2001) **87** 023201.

[22] M. Walter and J. Briggs. *J. Phys. B: At. Mol. Opt. Phys.* (1999) **32** 2487.

[23] M. S. Schoffler, K. Kreidi, D. Akoury, T. Jahnke, *et al. Phys. Rev. A* (2009) **78** 013414.

[24] L. Nagy, S. Borbély, and K. Póra. *Phys. Lett. A* (2004) **327** 481–489.

[25] D. Misra, A. H. Kelkar, S. Chatterjee, and L. C. Tribedi. *Phys. Rev. A* (2009) **80** 062701.

[26] L. Nagy, S. Borbély, and K. Póra. *Braz. J. Phys.* (2006) **36** 511.

[27] S. Borbély and L. Nagy. *Rad. Phys. Chem.* (2007) **76** 516.

[28] S. Borbély, K. Póra, and L. Nagy. *J. Phys.: Conf. Ser.* (2009) **163** 012067.

[29] V. D. Rodríguez, P. Macri, and R. Gayet. *J. Phys. B-At. Mol. Opt.* (2005) **28** 2775–2791.

List of Abbreviations

CTMC classical trajectory Monte Carlo method

CV Coulomb-Volkov

DVR discrete variable representation

FE finite element

FEDVR finite element discrete variable representation

HHG high harmonics generation

MPI multiphoton ionization

MSSFA momentum-space strong-field approximation

OBI over-the-barrier ionization

SAE single active electron approximation

SFA strong-field approximation

TDSE time dependent Schrödinger equation

TI tunneling ionization

VOLKOV Volkov model